Global Change Biology

Global Change Biology (2010) **16**, 171–186, doi: 10.1111/j.1365-2486.2009.01908.x

Remote sensing of sun-induced fluorescence to improve modeling of diurnal courses of gross primary production (GPP)

ALEXANDER DAMM*, JAN ELBERS†, ANDRÉ ERLER‡, BENIAMINO GIOLI§, KARIM HAMDI‡, RONALD HUTJES†, MARTINA KOSVANCOVA¶, MICHELE MERONI‖, FRANCO MIGLIETTA§, ANDRÉ MOERSCH‡, JOSE MORENO**, ANKE SCHICKLING††, RUTH SONNENSCHEIN*, THOMAS UDELHOVEN‡‡, SEBASTIAN VAN DER LINDEN*, PATRICK HOSTERT* and UWE RASCHER‡

*Geomatics Laboratory, Humboldt-Universität zu Berlin, Unter den Linden 6, 10099 Berlin, Germany, †Alterra, Duivendaal 2, 6701 AP Wageningen, The Netherlands, ‡Institute of Chemistry and Dynamics of the Geosphere, ICG-3: Phytosphere, Forschungszentrum Jülich, Stetternicher Forst, 52425 Jülich, Germany, §IBIMET-CNR, Istituto di Biometeorologia, Consiglio Nazionale delle Ricerche, Via G. Caproni 8, 50145 Firenze, Italy, ¶Laboratory of Plants Ecological Physiology, Division of Ecosystem Processes, Institute of Systems Biology and Ecology, Poříčí 3b, 60300 Brno, Czech Republic, ‖Remote Sensing of Environmental Dynamics Laboratory, DISAT, University of Milan-Bicocca, Piazza della Scienza 1, 20126 Milano, Italy, **Department of Earth Physics and Thermodynamics, University of Valencia, Dr Moliner, 50, 46100 Burjassot, Valencia, Spain, ††Institute for Geophysics and Meteorology, University of Cologne, Kerpener Str. 13, 50937 Cologne, Germany, ‡‡CRP-Gabriel Lippmann, Département 'Environnement et Agro-biotechnologies', Geomatic Platform, 41, rue du Brill, 4422 Belvaux, Luxembourg

Abstract

Terrestrial gross primary production (GPP) is an important parameter to explore and quantify carbon fixation by plant ecosystems at various scales. Remote sensing (RS) offers a unique possibility to investigate GPP in a spatially explicit fashion; however, budgeting of terrestrial carbon cycles based on this approach still remains uncertain. To improve calculations, spatio-temporal variability of GPP must be investigated in more detail on local and regional scales. The overarching goal of this study is to enhance our knowledge on how environmentally induced changes of photosynthetic light-use efficiency (LUE) are linked with optical RS parameters. Diurnal courses of sun-induced fluorescence yield (F_{Syield}) and the photochemical reflectance index of corn were derived from high-resolution spectrometric measurements and their potential as proxies for LUE was investigated. GPP was modeled using Monteith's LUE-concept and optical-based GPP and LUE values were compared with synoptically acquired eddy covariance data. It is shown that the diurnal response of complex physiological regulation of photosynthesis can be tracked reliably with the sun-induced fluorescence. Considering structural and physiological effects, this research shows for the first time that including sun-induced fluorescence into modeling approaches improves their results in predicting diurnal courses of GPP. Our results support the hypothesis that air- or spaceborne quantification of sun-induced fluorescence yield may become a powerful tool to better understand spatio-temporal variations of fluorescence yield, photosynthetic efficiency and plant stress on a global scale.

Nomenclature:

A_{max} =	maximum assimilation rate of CO_2 ($\mu mol\, CO_2\, m^{-2}\, s^{-1}$)
APAR =	absorbed photosynthetic active radiation ($\mu mol\, m^{-2}\, s^{-1}$)
CEFLES2 =	joint ESA campaign for the projects CarboEurope, Fluorescence Explorer, Sentinel2
Chl-F =	chlorophyll fluorescence
CO_2 =	carbon dioxide

Correspondence: Alexander Damm, tel. + 41 (0) 44 63 55 251, e-mail: alexander.damm@geo.uzh.ch

EC = eddy covariance
ESA = European Space Agency
ETR = photosynthetic electron transport rate ($\mu mol\, m^{-2}\, s^{-1}$)
ETR_{PAM} = electron transport rate measured with PAM fluorometer ($\mu mol\, m^{-2}\, s^{-1}$)
fAPAR = fraction of absorbed photosynthetic active radiation (%)
FLD = Fraunhofer line discrimination
F_T = terminal fluorescence measured with PAM fluorometer (AU)
F_O = minimum fluorescence measured with PAM fluorometer (AU)
$F_{M'}$ = maximum fluorescence of light-adapted leaf measured with PAM fluorometer (AU)
F_M = maximum fluorescence of dark-adapted leaf measured with PAM fluorometer (AU)
F_v = variable fluorescence of dark-adapted leaf measured with PAM fluorometer (AU)
F_v/F_M = maximum quantum yield of PS II of dark-adapted leaf (AU)
FOV = field of view
F_S = sun-induced fluorescence measured with spectrometer ($\mu mol\, m^{-2}\, s^{-1}$)
F_{Syield} = fluorescence yield measured with spectrometer (AU)
G = ground heat flux ($W\, m^{-2}$)
G_s = stomatal conductance ($mol\, H_2O\, m^{-2}\, s^{-1}$)
GPP = gross primary production ($\mu mol\, m^{-2}\, s^{-1}$)
GPP_{EDDY} = gross primary production measured with eddy flux tower ($\mu mol\, m^{-2}\, s^{-1}$)
GPP_{PRI} = gross primary production modeled with PRI ($\mu mol\, m^{-2}\, s^{-1}$)
GPP_{FS} = gross primary production modeled with sun-induced fluorescence ($\mu mol\, m^{-2}\, s^{-1}$)
$GPP_{F_{Syield}}$ = gross primary production modeled with fluorescence yield ($\mu mol\, m^{-2}\, s^{-1}$)
GPP_{const} = gross primary production modeled with a constant LUE ($\mu mol\, m^{-2}\, s^{-1}$)
H = sensible heat flux ($W\, m^{-2}$)
H_2O = water
J_{CO_2} = leaf-level CO_2 assimilation rate measured using the clip-on LICOR gas-exchange analyzer ($\mu mol\, m^{-2}\, s^{-1}$)
LAI = leaf area index ($m^2\, m^{-2}$)
LE = latent heat flux ($W\, m^{-2}$)
LED = light emitting diode
LUE = light-use efficiency ($mol\, CO_2\, mol^{-1}$ photons)
LUE_{EDDY} = light-use efficiency derived from eddy flux data ($mol\, CO_2\, mol^{-1}$ photons)
LUE_{LICOR} = light-use efficiency derived with LICOR gas-exchange analyzer ($mol\, CO_2\, mol^{-1}$ photons)
LUE_{PAM} = actual quantum efficiency or quantum yield of PS II measured with PAM fluorometer
NEE = net ecosystem exchange ($\mu mol\, m^{-2}\, s^{-1}$)
NPQ = nonphotochemical quenching
O_2 = oxygen
PPFD = photosynthetic photon flux density ($\mu mol\, m^{-2}\, s^{-1}$)
PRI = photochemical reflectance index
R_{eco} = ecosystem respiration rate ($\mu mol\, m^{-2}\, s^{-1}$)
PS I = photosystem I
PS II = photosystem II
RMSE = root mean square error
R_n = net radiation ($W\, m^{-2}$)
RS = remote sensing
u^* = friction velocity ($m\, s^{-1}$)
VPD = vapor pressure deficit (kPa)

Keywords: diurnal carbon uptake, eddy covariance, fluorescence yield, GPP, LUE, PRI, remote sensing, spectroscopy, sun-induced fluorescence

Received 8 December 2008 and accepted 11 February 2009

Introduction

Up to 90% of the gas exchange between the terrestrial bio-geosphere and the atmosphere is mediated by plants (Ozanne *et al*., 2003). Thereby, approximately 60 Gt of carbon are annually absorbed through plant photosynthesis (Janzen, 2004). Slight alterations within the terrestrial carbon balance can have significant impact on atmospheric carbon dioxide (CO_2) concentrations (Hilker *et al*., 2008b). In consequence, much effort in bio-geoscience research has been put in improving the understanding of CO_2 fluxes at different temporal and spatial scales (Baldocchi, 2003; Cohen *et al*., 2003; Turner *et al*., 2003a). Gross primary production (GPP) was identified as a key parameter to explore and quantify carbon fixation by plant ecosystems at various scales (Field *et al*., 1995; Goetz & Prince, 1999).

Currently, two different data-driven approaches exist to quantify variations in GPP at local or regional scales. (i) The eddy covariance (EC) technique aims at direct measurements of CO_2 net fluxes above canopies and uses micrometeorological methods to derive CO_2 exchange associated to a spatially extended footprint. (ii) Remote sensing (RS)-based approaches aim for air- and spaceborne retrieval of optical parameters that are related to photosynthetic carbon fixation.

An extensive network of EC towers was established during the last few decades. It provides CO_2 flux data from a wide range of plant ecosystems at high-temporal resolution (Baldocchi *et al*., 2001). Recent algorithmic development allows GPP estimates with high accuracy (Goulden *et al*., 1996; Baldocchi, 2003). EC towers measure carbon fluxes associated with a footprint area typically in the order of up to $\sim 1\,km^2$ depending on local setup and aerodynamic properties. Thus, measurements are local and solely representative for the underlying ecosystem as a whole (Turner *et al*., 2003b; Drolet *et al*., 2008).

RS offers the unique possibility to derive spatially explicit information on local, regional or global scales (Goetz & Prince, 1999; Freedman *et al*., 2002; Hilker *et al*., 2008b). Observations of GPP from RS is based on a relationship between spectral reflectance and two key vegetation parameters: the absorbed photosynthetic active radiation (APAR) and the plant efficiency to utilize this radiation for photosynthesis (Goetz & Prince, 1999). Monteith's (1972, 1977) mechanistic light-use efficiency (LUE) concept relates the photosynthetic capacity to LUE ($mol\,CO_2\,mol\,photons^{-1}$), defined as biomass production per unit absorbed light. Accordingly, knowing the incident PAR, GPP can be described as a function of the fraction of absorbed photosynthetic active radiation (fAPAR) and LUE (Turner *et al*., 2003a; Hilker *et al*., 2008b). Both parameters are highly variable and depend on phenological status, canopy structure and species composition (Field *et al*., 1995; Goetz & Prince, 1999). While fAPAR is expected to change mainly as a function of sun zenith angle and vegetation cover, LUE is highly dynamic and as a result, insufficient parameterization of this quantity is identified as a main source of uncertainty in modeling GPP (Turner *et al*., 2003b). In fact, plant photosynthesis is a dynamically regulated process that quickly adapts to environmental conditions and is affected by the ecological plasticity of each species (Turner *et al*., 2003b; Rascher & Nedbal, 2006). Consequently, LUE may greatly vary between different species and, additionally, is dynamically adjusted in diurnal and seasonal cycles (Schurr *et al*., 2006).

The observation of GPP from space can principally be grouped into three approaches: (i) methods that link optical vegetation indices to APAR with constant LUE; (ii) methods that are similar to the first one while LUE is related to meteorological parameters; (iii) approaches that estimate both APAR and LUE directly from RS data. The first two groups of methods often yields insufficient results, because they measure only APAR while assuming LUE to be constant or it is modeled from ancillary meteorological variables (Goetz & Prince, 1999; Grace *et al*., 2007). In this case, LUE is empirically related to some key meteorological variables such as temperature or vapor pressure deficit (VPD), which are selected as proxies for environmental stress (Field *et al*., 1995; Heinsch *et al*., 2003). Some studies show the potential of these approaches to predict GPP on regional and global scale with a temporal resolution of a couple of days (Heinsch *et al*., 2003; Running *et al*., 2004; Coops *et al*., 2007). However, such methods require frequent recalibration, being a limiting factor for long-term monitoring (Turner *et al*., 2005).

Research has recently focused on estimating APAR and LUE directly from RS data because these methods are expected to provide more realistic GPP estimates (Goetz & Prince, 1999; Grace *et al*., 2007). The peculiarity of this group of methods is that RS data are used to track the complex physiological process of photosynth-

esis and its strong dependency on different environmental conditions. The efficiency of photosynthesis is controlled on various levels, e.g. for chloroplasts, cells and leaves, in response to physiological characteristics and environmental conditions [see Schulze & Caldwell (1995) for a summary on the ecophysiology of photosynthesis]. In the case of limited photosynthesis and an increased amount of incident light, this excess energy can lead to photo-oxidative damages of the photosynthetic apparatus (Demmig-Adams & Adams, 1996; Baker, 2008). Two processes within the photosystem II (PS II) are known in dissipating the destructive energy and protecting the chloroplasts from damages. Fluorescence transforms the excess energy harvested at a given wavelength to emitted light at longer wavelengths (F_S). Nonphotochemical quenching (NPQ) mechanisms protect the chloroplasts by degrading the excess energy into heat (Demmig-Adams & Adams, 1996; Baker, 2008).

In the past years, relevant advances in sensor technology allowed to quantify LUE indirectly by remotely sensing of the two dissipation pathways – NPQ and fluorescence. The photochemical reflectance index (PRI) was designed to track the NPQ-related xanthophyll cycle at leaf level (Gamon *et al*., 1992, 1993). This important process within NPQ has a short response time to variable states of photosynthetic rates. Excessive light conditions induce the de-epoxidation of violaxanthin pigments into antheraxanthin and zeraxanthin – a mechanism reversible under low light conditions. The variable pigment composition leads to changes of the spectral signal at 531 nm (Gamon *et al*., 1992). PRI has been used in a variety of case studies and positively correlates with photosynthetic efficiency. It has been used successfully to detect changes in photosynthetic efficiency at the leaf level [see Rascher *et al*. (2007) for an overview of the literature]. However, PRI values greatly vary between species with the same photosynthetic capacity (Guo & Trotter, 2004). Additionally, canopy level PRI is strongly affected by viewing and illumination angles, soil background, leaf orientation and leaf area (Barton & North, 2001; Hilker *et al*., 2008b). Thus, the suitability of PRI as proxy for LUE in complex canopies remains unclear. Methy (2000) did not find a significant relationship of PRI and LUE at canopy level, whereas some studies have demonstrated the potential of PRI as proxy for LUE [see Hall *et al*. (2008) for a review on the subject].

Light energy absorbed by photosynthetic pigments is partly re-emitted as F_S, having well-defined spectral characteristics. Chlorophyll fluorescence (Chl-F) is emitted in two broad bands with peaks at about 685 and 740 nm (Lichtenthaler & Rinderle, 1988; Franck *et al*., 2002). The intensity of the fluorescence signal is in principle inversely correlated to the energy used for photosynthesis and thus can serve as an indicator for photosynthetic light conversion (Baker, 2008). However, the inverse correlation is in many cases lost as a result of increased rates of NPQ processes that become dominant in dissipating the excess energy (Govindjee, 1995) and the exact relationship between NPQ and fluorescence is hard to obtain (Maxwell & Johnson, 2000). Since commercial instruments for measuring fluorescence have become available in the past decades, the fluorescence method has been widely used in plant ecophysiological research on the level of single leaves and organs (Schreiber & Bilger, 1993; Schreiber *et al*., 1995).

In contrast to a detailed understanding on the level of single leaves, our research focused on investigating fluorescence-based methods for quantifying canopy level GPP, which requires remote analysis from above canopy. Recent studies showed that sun-induced Chl-F can principally be detected using passive techniques (Moya *et al*., 2004; Louis *et al*., 2005; Meroni & Colombo, 2006) and that remotely derived fluorescence signals and photosynthetic rates can be linked (Freedman *et al*., 2002; Louis *et al*., 2005; Meroni *et al*., 2008a, b). However, the sun-induced fluorescence signal and the relationship of fluorescence and LUE are not yet fully understood (Grace *et al*., 2007).

Operational methods solely rely on potential photosynthetic rates that were modified by microclimatological variables. Compared with such methods, approaches based on direct measurements of photosynthetic rates will simplify estimating GPP from RS data. Nevertheless, the measurement of parameters related to photosynthetic capacity with optical parameters is challenging. Hence, the overarching goal of this study is to further improve our understanding of LUE temporal dynamics, their linkage to environmental boundary conditions and the possibility to track these dynamics with optical parameters. Fluorescence yield and PRI were tested as proxies for LUE and their ability to explain short time responses of photosynthetic activity to environmental stress was investigated. Diurnal courses of radiometric measurements were acquired and the optical parameters *sun-induced fluorescence yield*, and *PRI* were derived. They were then used to predict GPP based on Monteith's LUE concept and compared with estimates from a local EC tower.

Materials and methods

Study site

Field data were acquired as part of the European Space Agency (ESA) supported CEFLES-2 campaign in June and September 2007 (http://www.esa.int/esaLP/

SEMQACHYX3F_index_0.html). The campaign was carried out in the 'Les Landes' area in southwest France. The main site is located near the commune Marmande, in a plain of the Garonne valley and dominated by intensive agriculture. Main crop types are corn (*Zea mays*), winter wheat (*Triticum vulgare*) and beans (*Phaseilus vulgaris*). An eddy flux tower (latitude/longitude 44.464, 0.196, altitude 22 m a.s.l.) was installed within a large corn field (500 m × 300 m), which was also mainly surrounded by corn fields.

The spectral database available for this research contains discontinuous time series of observations. During the first measurement period in June (1 day of measurements), corn was in the growing phase with an average plant height of 2 m. In September, when subsequent measurement periods 2 (3 days) and 3 (1 day) were undertaken, corn plants reached maximum heights of about 3.2 m and were at the beginning of the senescence phase. During both campaigns, the corn field was not irrigated.

Physiological data at leaf level

Leaf-level measurements using a pulse-amplitude-modulated (PAM) fluorometer, a gas-exchange analyzer and a chlorophyll meter were taken to verify potential physiological limitations of photosynthesis and to support interpreting canopy signals.

PAM fluorometry in the field. Chl-F measurements over corn leaves exposed to ambient incident photosynthetic photon flux density (PPFD) were performed with the miniaturized PAM (Heinz Walz GmbH, Eichenring, Effeltrich, Germany) with a leaf clip holder as described by Bilger *et al*. (1995). Fluorescence was excited by a pulsed modulated red light from a light emitting diode (LED), which passes a cut-off filter ($\lambda < 670$ nm, Balzers DT Cyan special, Optics Balzers AG, Lichtenstein). Terminal fluorescence (F_T) was determined at ambient light conditions. To determine maximum fluorescence ($F_{M'}$), a saturating light pulse (800 ms, $\sim 3000\,\mu mol\,m^{-2}\,s^{-1}$) was superimposed to the ambient light conditions.

Measurements were performed on September 13, 2007 for six individual plants in the same field, whereas two leafs per plant were measured from 09:30 hours until 15:45 hours. The values were aggregated for 1 h and 15 min time periods.

Actual quantum efficiency of PS II (LUE_{PAM}) (quantum yield of PS II) was calculated according to Genty *et al*. (1989) as

$$LUE_{PAM} = \frac{F_{M'} - F_T}{F_{M'}} = \frac{\Delta F}{F_{M'}}. \quad (1)$$

The photosynthetic electron transport rate measured with PAM fluorometer (ETR_{PAM}) was obtained as follows:

$$ETR_{PAM} = \frac{\Delta F}{F_{M'}} \times PPFD \times 0.5 \times 0.84. \quad (2)$$

The use of the factor 0.5 assumes that the incident quanta were used to excite both PS II and PS I. The value 0.84 accounts for the absorption coefficient of leaves. As this factor is not exactly known for corn, we used the empirical mean absorption factor (Ehleringer, 1981). PPFD of each leaf area unit was obtained with a leaf clip holder featuring an integrated microquantum sensor.

Maximum or potential quantum yield of PS II (F_v/F_M) was calculated according to the following equation:

$$F_v/F_M = \frac{(F_M - F_O)}{F_M}, \quad (3)$$

where F_M denotes the maximum fluorescence of the dark-adapted leaf when a saturating light pulse of 800 ms duration (intensity $\sim 3000\,\mu mol\,m^{-2}\,s^{-1}$) was applied.

Gas exchange measurements. Light response curves of CO_2 assimilation rate (J_{CO_2}) were measured using the LED light source Li-6400-02B (LiCor, Lincoln, NE, USA). The values of J_{CO_2} were recorded with a gas-exchange system Li-6400 (LiCor). The irradiances used for the light response curve were 0, 80, 250, 600, 1200 and 1800 μmol photons $m^{-2}\,s^{-1}$. This measuring protocol allowed the estimation of J_{CO_2} at a given PPFD as half-hour averages of the eddy flux measurements.

Measurements were performed on September 12, 2007 from 07:30 hours until 17:30 hours on four individual plants. The CO_2/H_2O fluxes were measured as an integral signal from the central parts of the leaves (investigated area 6 cm^2) on the fourth leaves from the top. The leaves were kept inside the assimilation chamber under constant CO_2 concentration ($380 \pm 5\,\mu mol\,CO_2\,mol^{-1}$), air humidity and leaf temperature (outdoor ambient) during the measurement. Air flow rate through the assimilation chamber was maintained at 500 $\mu mol\,s^{-1}$.

LUE_{LICOR} was derived as the ratio of J_{CO_2} and PPFD given as a half-hour average from the eddy flux measurements.

Chlorophyll content. The leaf chlorophyll content was measured with the Chlorophyll Meter SPAD-502 (Spectrum Technologies Inc., Plainfield, IL, USA). The relative measurements of the SPAD device were calibrated using laboratory chlorophyll extractions. For this purpose, leaf disks were cut with a standardized cork borer, placed in plastic tubes and

stored in liquid nitrogen. The chlorophyll content of the leaf samples was extracted in the laboratory using the method after Lichtenthaler (1987).

Physiological data at canopy level

Net ecosystem exchange (NEE) was measured half-hourly (EC tower) from April until September 2007 together with friction velocity (u^*), energy fluxes and fluxes of trace species. Sensible heat flux (H), latent heat flux (LE) and ground heat flux (G) were measured to calculate the surface energy balance expressed as the distribution of net radiation (R_n). Standard equipment included a 3D sonic anemometer, an infrared gas analyzer measuring CO_2 and gaseous H_2O mass densities at high frequency, a slow response infrared gas analyzer measuring vertical CO_2 concentration profiles at five levels up to 20 m, a soil heat flux plate, and global and net radiation sensors. u^*, H, LE and NEE were calculated using the EC technique, following the standardized protocol for instrument setup and data processing by Aubinet *et al*. (2000), including density corrections for open path gas analyzers (Webb *et al*., 1980).

Raw flux data required additional preprocessing for reliable subsequent analyses (Goulden *et al*., 1996). Three preprocessing steps were performed using a set of algorithms provided by the CarboEurope network (CarboEurope 2008) and described elsewhere (Papale & Valentini, 2003; Reichstein *et al*., 2005). Because EC measures the NEE (i.e. the sum of CO_2 fixed by plants, GPP and ecosystem respiration rate, R_{eco}), the integrated flux signal was partitioned to derive GPP. For this purpose, night-time NEE measurements were used to relate R_{eco} to soil temperature. Day time R_{eco} was obtained with the established relationship and subtracted from the daytime NEE values.

Finally, the preprocessed data were smoothed using a 1.5 h moving window filter to reduce data inherent noise (Reichstein *et al*., 2002; Eiden *et al*., 2007). Besides GPP, light-use efficiency derived from eddy flux data (LUE_{EDDY}) was calculated as second reference parameter from the EC data. LUE_{EDDY} was derived as ratio of GPP_{EDDY} and PPFD according to Wofsy *et al*. (1993).

Remotely sensed data and optical parameters

A FieldSpec Pro III high-resolution spectroradiometer (Analytical Spectral Devices, Boulder, CO, USA) (ASD, 2002) was installed at 30 m distance to the eddy flux tower to measure diurnal cycles of canopy radiometric response. It registers reflected radiation within the spectral domain of 350–2500 nm with a nominal bandwidth of 1.4 nm (350–1050 nm) and a field of view (FOV) of 25°. A calibrated Spectralon™ panel (0.25 m × 0.25 m) was used for calibration of the instrument and to measure incident irradiance.

The instrument's fiber optic was mounted on a robotic arm of 0.6 m length, approximately 1 m above the canopy. Moving the robotic arm allowed an automatic collection of daily cycles of spectral reflectance at four different locations, each of which was 0.5 m in diameter (Fig. 1). The acquired dataset consists of spectral records from four canopy areas, bracketed by measurements of the reference panel. At each position, 10 single spectra were recorded and each spectrum was averaged from 25 individual measurements. Integration time was automatically optimized during the day in order to maximize the signal-to-noise ratio.

Five diurnal courses were acquired during the campaign that covers two different phenological periods, June and September 2008 (Table 1). Measurements acquired in September were collected in two different locations of the same field and therefore they were divided into two datasets and treated separately. Hence, period one corresponds to a single day course in June. Period two consists of three diurnal courses from the 5th to 7th of September. Period three corresponds to measurements from the 12th of September at a different position in the same field.

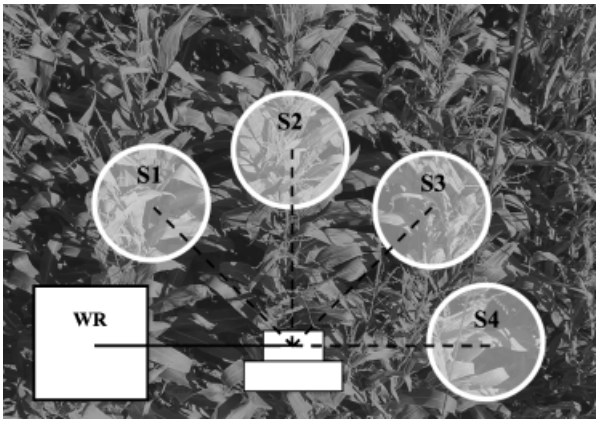

Fig. 1 Position and dimension of spectrometer footprint (S1–S4) for a corn at average canopy height. The position of the white reference panel (WR) is also indicated.

Table 1 Summary of available day courses of radiometric measurements of a corn canopy

Period	Date	Time window (hh:mm, UTC)
1	June 30	14:30–19:30
2	September 5	10:30–18:00
2	September 6	09:00–17:00
2	September 7	09:30–18:00
3	September 12	09:00–16:50

The PRI was introduced by Gamon *et al*. (1992) to track the epoxidation state of the xanthophyll pigments. The index is based on two wavelengths in the visible spectral domain. The spectral reflectance at 531 nm (R_{531}) is sensitive for pigment variation associated to NPQ while the reflectance at 570 nm (R_{570}) is used as reference. The PRI was derived as:

$$\mathrm{PRI} = \frac{R_{531} - R_{570}}{R_{531} + R_{570}}. \quad (4)$$

Reflectance values were calculated using the Spectralon™ (Labsphere, North Sulton, NH, USA) reference measurements.

The amount of sun-induced Chl-F (F_S) emitted by a sunlit leaf is only 1–5% of the total reflected light at a certain wavelength, which complicates quantifying the fluorescence signal from RS observations. However, the solar light is absorbed in the solar or earth atmosphere at the so-called *Fraunhofer lines* and no or strongly reduced incoming radiation reaches the Earth surface. Fluorescence originated in the canopy also occurs in the otherwise 'black' absorption bands and, therefore, can be selectively quantified. Solar irradiance at ground level exhibits three main absorption bands in the red and near-infrared spectral domain: the H_α line at 656.3 nm is due to the hydrogen absorption by the solar atmosphere whereas two bands at 687 nm (O_2-B) and 760 nm (O_2-A) are due to the molecular oxygen absorption by the terrestrial atmosphere. Especially the O_2-A and -B bands overlap with the Chl-F emission spectrum and are wide enough to allow quantifying fluorescence from air- and spaceborne platforms. The Fraunhofer line discrimination (FLD) method has been proposed for this purpose (Plascyk, 1975) and was used with success in different works (Carter *et al*., 1990; Moya *et al*., 2004).

In this study, we used the O_2-A band, which is the widest of the three absorption bands (deepest absorption at 760 nm, <2 nm bandwidth; maximum bandwidth affected by O_2 absorption ~ 12 nm), to quantify fluorescence according the modified FLD method proposed by Maier *et al*. (2003). This approach assumes that F_S is additive to the reflected signal and can be derived by comparing the depth of the oxygen absorption band at 760 nm from a nonfluorescent surface with that of the fluorescent vegetation target according to the following equation:

$$F_S = \frac{L_1 - \frac{E_1}{E_2} L_2}{1 - \frac{E_1}{E_2}}, \quad (5)$$

where E is the radiance upwelling from the nonfluorescent target, L is the radiance of vegetation, and the subscripts 1 and 2 indicating the wavelengths within and outside of the absorption line, respectively. We employed the band at 760 nm for E_1 and L_1 and an average of the spectral bands at 745–755 and 770–785 nm for E_2 and L_2.

Besides responding to photosynthetic status, fluorescence is also driven by the absolute magnitude of the incident irradiance. Hence, it is necessary to normalize the estimated F_S signal to get a fluorescence yield independent of the light level. This can be achieved by dividing the number of photons emitted (F_S) and the number of photons absorbed by the plants (APAR). The resulting signal is termed fluorescence quantum yield (F_{Syield}) (Govindjee, 2004) and can be related to the photosynthetic efficiency (Louis *et al*., 2005) and was obtained according to the following equation:

$$F_{Syield} = \frac{F_S}{\mathrm{APAR}}. \quad (6)$$

GPP modeling

For modeling GPP based on RS data, we used the concept introduced by Monteith (1972, 1977). According to Eqn (7), GPP is a function of APAR and LUE:

$$\mathrm{GPP} = \mathrm{APAR} \times \mathrm{LUE}. \quad (7)$$

APAR was obtained from the radiometric measurements as integrated difference between the incident and reflected radiance in the spectral region from 400 to 700 nm (Zhanqing & Moreau, 1995), thus neglecting the absorption of the background (i.e. dry and bright bare soil). LUE was empirically modeled on the basis of the optical parameters F_{Syield} and *PRI* to investigate their potential to track physiological variations in the photosynthetic apparatus that determine LUE.

The measured radiometric signal is a function of biochemical, structural and viewing/illumination parameters (Goel, 1989). All these factors have to be considered in order to establish a relationship between the optical parameters and LUE. We used a simple approach to account for structural changes in the canopy during the growing season. This approach consists of performing an empirical analysis period by period along the vegetation cycle in a way that it is reasonable to assume that no major structural changes occur within a given period. Therefore, for each of the three measurement periods, a linear transfer function was established between the optical parameter and LUE_{EDDY}.

Validation of the modeled GPP was performed exploiting measured GPP values from EC (GPP_{EDDY}). The footprint of the tower depends on various environmental and surface conditions as well as the instrumental setup (height of the tower) and can range between a few

hectares to a few square kilometers (Schmid & Lloyd, 1999). The area to which the flux measurements are most sensitive, the so called *footprint peak*, is smaller and typically extends upwind the measurement point for a distance of few hundred meters (Kljun *et al.*, 2004). The results from an analytical footprint model (Hsieh *et al.*, 2000) indicate that the peak footprint is mostly located within the corn field (maximum peak distance of 170 m) and the performed comparison with radiometric measurements within the corn field is hence feasible (Hilker *et al.*, 2008a).

Results

Measurements of CO_2 exchange and active fluorometry at leaf level show a physiological limitation of photosynthesis during the days in September. Figure 2a shows LUE over the course of one day (September 13) measured at different levels: (1) leaf-level LUE of light reactions of photosynthesis was measured using the clip-on PAM fluorometer (LUE_{PAM}), (2) leaf-level LUE of carbon fixation was measured using the clip-on LICOR gas-exchange analyzer (LUE_{LICOR}) and (3), for comparison, canopy-level LUE of carbon fixation was derived from the eddy flux data (LUE_{EDDY}). Even though leading to different absolute values, the three measurements showed a comparable diurnal course with high LUE during environmentally moderate morning hours, a clear depression of LUE during afternoon, when conditions are dry and hot, and an increase toward the evening, when conditions again become moderate. Additionally, leaf-level LUE began to increase around 12:30 hours, while canopy LUE recovery was delayed by about 2 h (Fig. 2a). We compared photosynthetic rates at the three levels (Fig. 2b): (1) leaf-level electron transport rate at PS II was measured using the clip-on PAM fluorometer (ETR_{PAM}), (2) leaf-level CO_2 uptake rate was measured using the clip-on LICOR gas-exchange analyzer (J_{CO_2}) and (3) canopy-level GPP was derived from the eddy flux data (GPP_{EDDY}). Regardless the used method, maximum rates of photosynthesis occurred between 10:00 and 12:00 hours, when PPFD also reached its maximum. During afternoon, photosynthetic rates decreased and the time shift between leaf and canopy-level measurements is observable again: $ETR_{PAM,}$ referring to the very first step of photosynthetic energy conversion (light reaction), decreases first, followed by a decrease in the leaf-level CO_2 uptake rate (J_{CO_2}, dark reactions), and finally also ecosystem GPP_{EDDY} decreased (Fig. 2b).

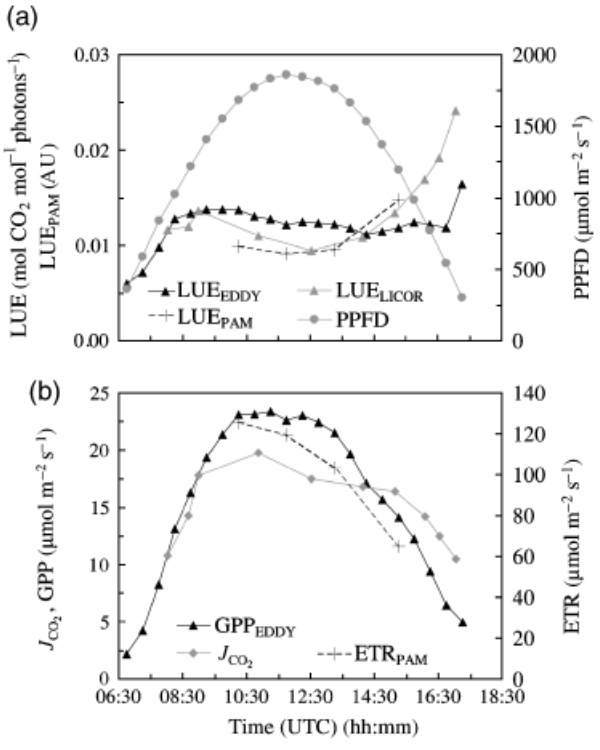

Fig. 2 Comparison of diurnal courses of leaf and canopy LUE and GPP of corn at the 13th of September. (a) Incident PPFD and LUE estimated from different sources: canopy-level eddy flux measurements, LUE_{EDDY}; leaf-level gas exchange, LUE_{LICOR}; and leaf-level active fluorometry, LUE_{PAM}. (b) Production related information as estimated from eddy flux measurements, GPP_{EDDY}; gas exchange, J_{CO_2}; and active fluorometry, ETR_{PAM}. PPFD, photosynthetic photon flux density; LUE, light use efficiency; GPP, gross primary production.

The time shift between leaf and canopy measurements can be explained by the vertical characterization of the canopy showing significant variations of parameters related to photosynthesis (Fig. 3). The canopy was in the beginning of the senescent phase in September and grain filling was still in progress. Corn canopies in this phenological state are affected by senescing effects spreading in two different directions: a decline of structural and functional parameters from top to bottom and from bottom to top (Tollenaar & Daynard, 1978; Valentinuz & Tollenaar, 2004). Both directions can be observed with our measurements. The structural parameter *chlorophyll content* was highest for the middle leaves (45–50 $\mu g\,cm^{-2}$) and largely decreases for the upper leaves (20–35 $\mu g\,cm^{-2}$) (Fig. 3, left panel). A similar trend was measured for different functional parameters. The highest values for the maximum assimilation rate of CO_2 (A_{max}) and the stomatal conductance (G_s) (Fig. 3, middle panels) were observed for the middle leaves, whereas both parameters declined in upward and downward directions. On the contrary, the maximum quantum yield of PS II (F_v/F_M) shows a monotonous decline from the bottom (0.77) to the top (0.72) (Fig. 3, right panel). Lower values in the upper

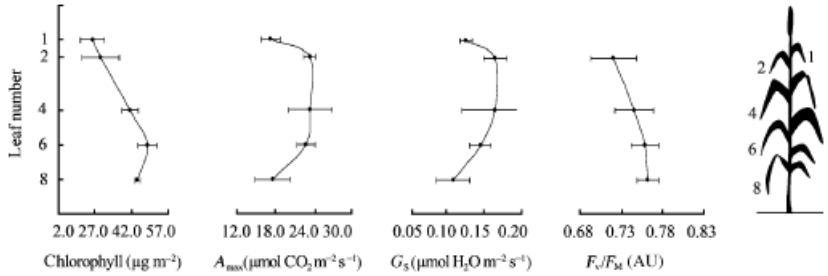

Fig. 3 Mean vertical distribution ($n = 3$ plants) of chlorophyll, maximum assimilation rate (A_{max}), stomatal conductance (G_s), and maximum quantum yield of PS II (F_v/F_M) for a senescent corn plants. Horizontal bars refer to $\pm$ 1 standard deviation. Vertical profiles were collected at the 13th of September and are expressed in term of leaf number, first and eighth leaves being the uppermost and the lowermost, respectively. The plant drawing on the right indicates the leaf vertical position. The decline of parameters from middle to top and middle to bottom is due to senescence (refer the text above for an explanation).

leaves which are more exposed to incident PPFD, together with the overall absolute value of $F_v/F_M < 0.77$ [healthy leaves have an F_v/F_M of 0.83 (Bjorkman & Demmig, 1987)] may indicate that the canopy was additionally affected by photoinhibition.

Eddy flux data for all days showed that the carbon fixation of plants is mainly determined by the amount of incident photosynthetic active radiation (Fig. 4a), which is in agreement with results documented in the literature (Wofsy *et al.*, 1993).

The assimilation rate in June (highest peak value 50 μmol $m^{-2} s^{-1}$) was higher than in September (highest peak value 32 μmol $m^{-2} s^{-1}$). The decrease in September was due to lower PPFD but also due to lower LUE (June: 0.057 mol CO_2 mol^{-1} photons; September: 0.031 mol CO_2 mol^{-1} photons) (Fig. 4b). In fact, seasonal differences in GPP_{EDDY} are not affected only by the incident PPD but also by the phenological state of the crop, which in turn determines leaf area index (LAI) and photosynthetic pigments in the canopy. In June, the canopy was in the growing phase (chlorophyll content 0.0105 μg m^{-2}, LAI 2.2) while in September it was at the beginning of the senescence phase (chlorophyll content 0.0093 μg m^{-2}, LAI 2.8).

Day courses of GPP_{EDDY} in June were symmetrical around solar noon, while in September GPP_{EDDY} data showed an asymmetry in the diurnal course with a clear depression in the afternoon (Fig. 4a). This phenomenon is often described as 'midday depression' and explained with high temperature and high vapor pressure difference (VPD) between air and leaf-tissue that often cause high evaporative demand. This in turn causes stomata to close and results in reduced carbon uptake around noon and early afternoon. Hence, under comparable illumination conditions the carbon uptake is reduced in the afternoon with respect to the morning hours.

We tested the validity of optical parameters (F_{Syield} and PRI) measured above the canopy for their potential

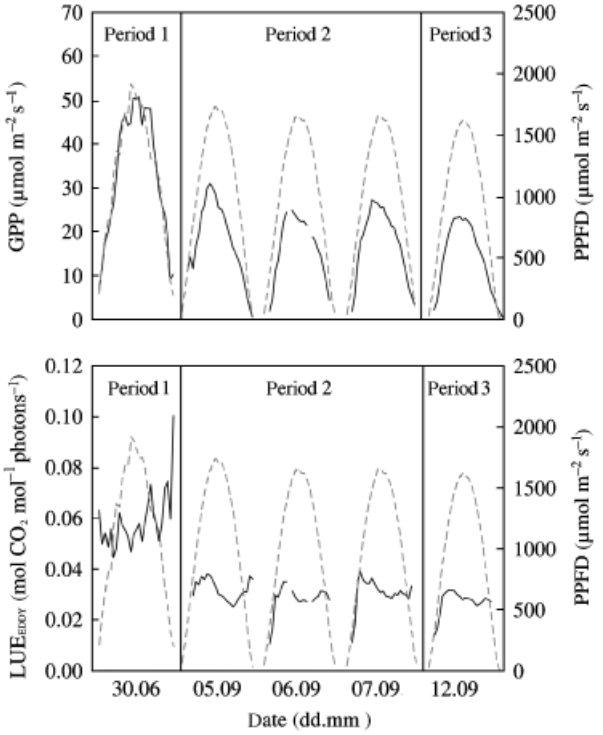

Fig. 4 Diurnal courses of GPP_{EDDY} [continuous curve, a (top)] and LUE_{EDDY} [continuous curve, b (bottom)] derived from eddy-flux measurements during the three measurement periods. Incident PPFD is reported for reference (dashed curve). GPP_{EDDY}, gross primary production measured with eddy flux tower; LUE_{EDDY}, light-use efficiency derived from eddy flux data; PPFD, photosynthetic photon flux density.

to quantify the dynamic changes in canopy LUE. Therefore, an empirical and linear transfer function between the optical parameters and LUE_{EDDY} was calculated for each time period and position within the field (Fig. 5a and c).

The relationships gathered by matching simultaneous measurements of LUE_{EDDY} and optical parameter were

weak for both optical parameters in all three periods (Table 2).

On the experimental basis of the time shift observed for LUE measured at different scales (i.e. leaf and canopy, see Fig. 2) we hypothesized that an analogous time shift may exists between canopy LUE (i.e. LUE_{EDDY}) and optical parameters. In order to find this time shift, we systematically adjusted the datasets for the time shift using a cross-correlation approach (Fig. 6). The relationship between the F_{Syield} and LUE_{EDDY} significantly increased by shifting F_{Syield} by −1.5 h (Figs 5b and d and 6 and Table 2).

Especially the time-shifted data show a stepwise increase of the multiplicative factors of the linear transfer functions between LUE_{EDDY} and F_{Syield} with ongoing senescence (Fig 5b). In contrast, even on time-shifted data, relationships for the PRI were weaker and no systematic trend was found (Fig. 5d).

Once the transfer functions for every single period were defined as above, we employed them in Eqn (7) (i.e. to model LUE) to estimate GPP daily courses of GPP in 30 min intervals. GPP estimated from fluorescence yield ($GPP_{F_{Syield}}$) showed the best agreement with the measured diurnal courses of GPP_{EDDY}, while using the PRI (GPP_{PRI}) did not yield reasonable estimates of GPP_{EDDY} (Fig. 7 and Table 3).

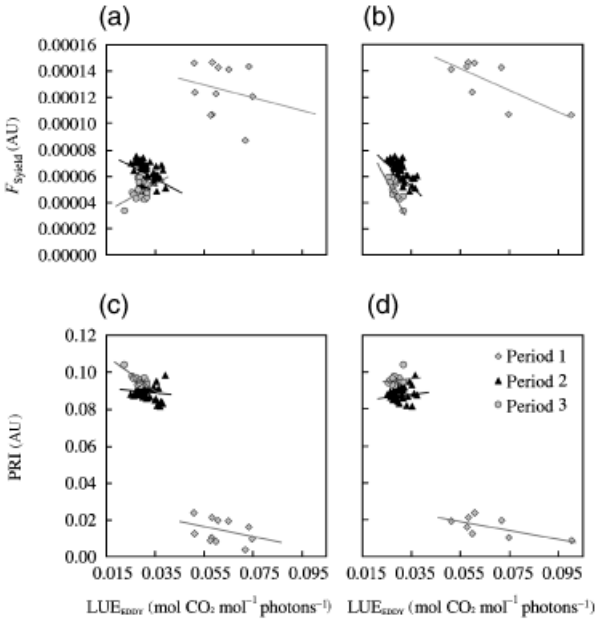

Fig. 5 Relationship between LUE_{EDDY} and optical parameters (fluorescence yield and PRI). (a, c) Relationship without time shift. (b, d) With time shift. Period 1 corresponds to the 30th of June, period 2 to the 5th to 7th of September and period 3 to the 12th of September. PRI, photochemical reflectance index; LUE_{EDDY}, light-use efficiency derived from eddy flux data.

Table 2 Statistical parameters characterizing the relationship of LUE_{EDDY} and optical parameters

	June	September 5–7	September 12	Average
R^2				
F_{Syield}	0.04	0.17	0.14	0.12
F_{Syield}_time	0.56	0.46	0.59	0.54
PRI	0.13	0.02	0.65	0.27
PRI_time	0.44	0.04	0.19	0.22
RMSE				
F_{Syield}	0.026	0.005	0.004	0.0117
F_{Syield}_time	0.013	0.005	0.001	0.0063
PRI	0.029	0.017	0.006	0.0173
PRI_time	0.060	0.018	0.003	0.0270
P-value				
F_{Syield}	0.99	0.06	0.38	0.48
F_{Syield}_time	0.40	0.96	0.46	0.60
PRI	0.98	0.30	0.99	0.76
PRI_time	0.95	0.94	0.86	0.92
N				
F_{Syield}	11	49	15	
F_{Syield}_time	8	31	14	
PRI	11	43	15	
PRI_time	8	31	14	

F_{Syield}, fluorescence yield; F_{Syield}_time, time shifted F_{Syield}; PRI, photochemical reflectance index; PRI_time, time shifted PRI; *P*-value, significance of correlation; *n*, number of measurements; LUE_{EDDY}, light-use efficiency derived from eddy flux data.

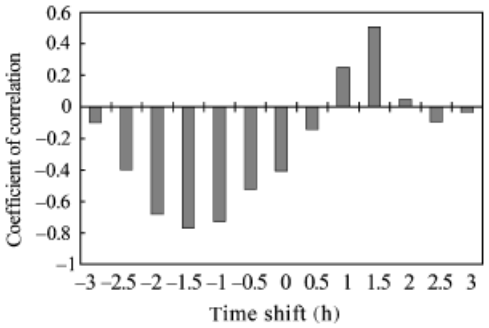

Fig. 6 Coefficients of determination (*R*) for cross-correlation-based time shift analysis. F_{Syield} were shifted against fixed LUE_{EDDY} data. F_{Syield}, fluorescence yield measured with spectrometer; LUE_{EDDY}, light-use efficiency derived from eddy flux data.

For sake of comparison Fig. 7 also reports GPP model assuming a constant LUE (computed as diurnal average of the LUE_{EDDY} values).

Discussion

The main focus of this study was to evaluate the use of optical parameters for modeling short time responses of

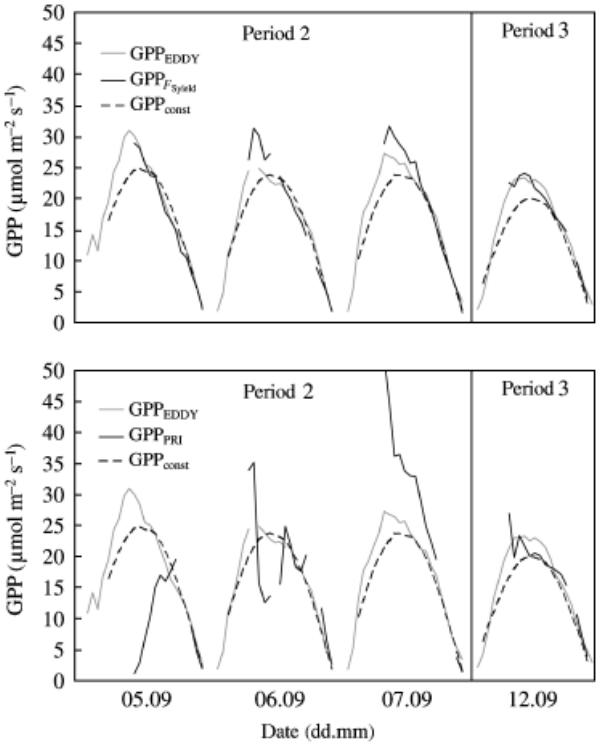

Fig. 7 Diurnal courses of modeled and measured GPP_{EDDY} signal. (a) $GPP_{F_{Syield}}$ based on fluorescence yield. (b) GPP_{PRI} based on PRI. GPP_{const} refers to GPP modeled with a constant LUE. PRI, photochemical reflectance index; GPP_{EDDY}, gross primary production measured with eddy flux tower; GPP_{PRI}, gross primary production modeled with PRI; GPP_{const}, gross primary production modeled with a constant LUE; LUE, light-use efficiency.

photosynthesis and CO_2 assimilation to environmental conditions. Therefore, diurnal courses of F_{Syield} and PRI were acquired and used as proxies for LUE.

Using basic Monteith's modeling (i.e. constant value for LUE) provided poor results: the amount of fixed CO_2 was underestimated in the morning and strongly overestimated from midday until afternoon. The use of PRI to modulate the LUE did not increase the accuracy of the estimates: the assimilation estimates based on PRI (GPP_{PRI}) did not even track the shape of the measured GPP_{EDDY} (Fig. 6). Sims *et al*. (2006) or Methy (2000) denote a significance decrease of the relationship between PRI and photosynthesis if measurements were upscaled from leaf to canopy level. In contrast, a couple of studies show that the PRI is sensitive for diurnal variations of canopy photosynthesis (e.g. Nichol *et al*., 2002; Hall *et al*., 2008). The situation remains unclear and requires more systematic research. However, Barton & North (2001), Grace *et al*. (2007) and Hilker *et al*. (2008a) demonstrated the dependency of the PRI on various structural effects and illumination conditions.

Table 3 Statistical parameters characterizing the relationship of modeled and measured GPP

	June	September 5–7	September 12	Average
R^2				
const. LUE	0.91	0.92	0.95	0.93
F_{Syield}	0.30	0.83	0.89	0.67
$F_{Syield\_}$ time	0.83	0.97	0.98	0.93
PRI	0.20	0.05	0.52	0.26
PRI_ time	0.52	0.34	0.87	0.58
RMSE				
const. LUE	4.42	2.51	1.48	2.80
F_{Syield}	12.40	2.75	2.15	5.77
$F_{Syield_}$time	4.55	1.91	0.97	2.48
PRI	13.20	11.40	3.15	9.25
PRI_time	7.39	10.94	7.98	8.77

F_{Syield}, fluorescence yield; $F_{Syield_}$time, time shifted F_{Syield}; PRI, photochemical reflectance index; PRI_time, time shifted PRI; const. LUE, constant light use efficiency; GPP; gross primary production.

Apparently, the diurnal dynamics of photosynthesis tracked with the PRI is affected by canopy structure and observation properties. The superimposition may amplify in stressed, photoinhibited canopies as shown in this study. In such cases, the dynamical adaptation of NPQ mechanisms is limited and appears more constant during the day. Nevertheless, our results show that the PRI is to some extent sensitive to seasonal variations, which is in consistency with other works (Nichol *et al*., 2002; Hall *et al*., 2008). Thus, the assumption of decreasing LUE_{EDDY} and PRI with increasing senescence can be confirmed in the seasonal context (Fig. 5c and d). Fluorescence yield, on the other hand, is capable of reproducing the diurnal course of GPP and the prominent midday depression (Fig. 7).

The time shift of 1.5 h between the flux and radiometric data can be mechanistically explained as follows: plant photosynthesis is primarily driven by the meteorological variables *water vapor deficit*, *temperature* and *photosynthetic photon flux density*. The diurnal variation of these variables leads to the midday depression of photosynthesis that is most prominent for C3 species but also present for C4 species (Hirasawa & Hsiao, 1999). However, it must be noted that not all the leaves composing the canopy experience the same environmental conditions during the day. For example, top level leaves will receive more radiation than bottom leaves. Moreover, as a result of the vertical gradient in environmental conditions (including radiation, temperature, VPD), the leaves adapt to different biochemical and physiological states, as demonstrated by the vertical characterization of the corn canopy described in

Fig. 3. The graph shows that the vertical variability of the meteorological variables leads to different photosynthetic rates and capacities within different layers of the canopy. This basically means that GPP of different canopy layers will respond to environmental conditions at different times during the day. GPP_{EDDY} in contrast will detect the overall response of the canopy.

The importance of such observations is confirmed by different models. Chen *et al*. (1999) showed, for example, an improvement of diurnal estimates of canopy photosynthesis using multilayer models instead of a one-layer model. The improvement was mostly due to the fact that multilayer models consider the vertical variability of photosynthesis.

In our experiment, the observed areas of the canopy differ within the FOV of the eddy flux tower and the spectrometer. The flux tower receives an integrated signal from a huge footprint and the entire vertical canopy. The spectrometer, however, observes the response from the upper canopy. This layer of the canopy is earlier exposed to high light intensities and high VPD than the lower ones. Additionally, the elevated senescence in the upper canopy and effects of photoinhibition leading to a higher stress level in the upper leaves compared with the leaves in the middle canopy (Fig. 3). Hence, it is likely that the stomatal conductance of the upper leaves is reduced earlier during the day than that of the other inner leaves. As a consequence, the modeled GPP based on optical parameters (sensing mainly the upper leaves) will decrease earlier than the measured GPP_{EDDY} from the integrated canopy.

This interpretation was supported by analyzing two diurnal courses of another crop (winter wheat) from early May 2008 (data not shown). The canopy was 0.30 m high and the conditions of different vertical layers of the canopy are expected to be more homogeneous. No time discrepancy between the eddy flux measurements and the optical parameters were observed in this case.

Besides the mentioned physiological explanation, also micrometeorological considerations can explain the observed time shift. Air masses might remain stored within the canopy some time before being grabbed by turbulent eddies that can be sampled by the EC technique.

The measured radiometric signal is a function of biochemical, structural and external factors and the absolute value of the derived optical parameters depend on these factors. Barton & North (2001) showed, for example, the dependency of PRI on LAI, leaf angle distribution, solar/view angle and soil type. As natural canopies are an assembly of differently oriented leaves, which change their orientation during plant development and as a response to environmental conditions, there is no general function available to transfer PRI or fluorescence yield into LUE (Barton & North, 2001). In this study, we used empirical transfer functions to scale the optical parameters to LUE_{EDDY} (Fig. 5). The negative correlation between F_{Syield} and LUE_{EDDY} seems reasonable as we found some indications for photoinhibition with a F_v/F_M of 0.75, especially for the upper leaves (Fig. 3). Under such photoinhibited circumstances, nonphotochemical mechanisms do not vary significantly and, hence, do not dynamically adapt to environmental conditions. In consequence, NPQ appears nearly constant during the day. LUE is reduced as a result of limited photosynthesis in such situations. At the same time, the F_{Syield} increases with increasing amount of incident photons and in consequence, the relationship appears negative (refer van der Tol *et al*., 2009, for a description based on a mechanistic model).

A change in the slope of the transfer functions between LUE_{EDDY} and F_{Syield} was observed in the two phenological stages considered. During the process of senescence, the amount of chlorophyll declines. Additionally, a higher stress potential can be expected in September due to unfavorable environmental and meteorological conditions (e.g. dry soils), which result in a stomata closure from late morning until early afternoon. The photosynthetic capacity of the plants is limited and stress occurs due to high light conditions. In such situations, photoprotection mechanisms were upregulated to dissipate the excessive light and avoid photoinhibition. In the case of chronicle photoinhibition, NPQ processes may be limited and an increased amount of light is converted to fluorescence light.

One of the crucial steps in such kind of analysis is the choice of a proper and robust retrieval method. We investigated different methods, e.g. the standard FLD method (Plascyk, 1975), the modified method proposed from Maier *et al*. (2003) and the improved FLD method from Alonso *et al*. (2008). The absolute values of F_S differed for all methods, but each of them provided a similar sensitivity to the diurnal variability of the fluorescence signal. Finally, we decided to use the method proposed from Maier *et al*. (2003) being most robust and less sensitive to errors occurring during the measurement of the fluorescence signal. We are aware of some of the restrictions of the method, especially the assumption of linearity and maybe a slight sensitivity to bidirectional reflectance effects.

Utilizing fluorescence to model GPP spatial explicit at regional or global scale, however, necessitates investigation on challenging issues. These are (i) the precise correction of atmospheric effects that are influencing the measurement of satellite-based fluorescence (Guanter *et al*., 2007); (ii) a better understanding of the influence of canopy structure at the F_S signal; (iii) contribution of different surface elements to the F_S signal covered with

a remote sensor; (iv) impact of changing viewing-illumination geometry to the F_S signal (Meroni *et al*., 2008b). A further research topic is the physiological relationship between fluorescence and photosynthesis. Various working groups showed a significant relationship between F_S and photosynthesis [van der Tol *et al*. (2009) as example for modeled data, or Meroni *et al*. (2008b) as example for experimental studies]. However, the existence of NPQ mechanisms may lead to changing relationships between both parameters within 1 day, between different species and in response to phenological states. The ESA supported global satellite mission for sensing solar-induced fluorescence FLEX (Fluorescence Explorer) is currently under evaluation. Within this framework, the mentioned aspects are subjects of research. For example, the recent availability of an integrated leaf-canopy fluorescence model [ESA, FluorMOD project (Zarco-Tejada *et al*., 2006)], in combination with mechanistic experimental field studies, should provide the necessary base for investigating the mentioned effects in order to upscale the approach to landscape level.

Conclusions and outlook

To our knowledge, this work shows for the first time the modeling of diurnal courses of GPP based on remotely sensed fluorescence yield. We showed that the short time response of a complex physiological process to variable environmental conditions can be tracked reliably with this optical parameter.

The correlation analysis between F_{Syield} and LUE_{EDDY} highlighted a time discrepancy between the two measurements (F_{Syield} anticipated LUE_{EDDY} by 1.5 h). Accounting for this delay was hence to correctly relate eddy flux measurements to remotely sensed estimates of LUE. An explanation of this delay related to the vertical structure of the canopy and to the different footprint sensed by the eddy and spectrometric systems was given. Nevertheless, the influence of the canopy structure on both eddy and spectrometry needs to be investigated in depth to fully understand its influence on GPP estimates from remotely sensed data.

We were able to account for the impact of structure on the radiometric signal with a straightforward empirical approach. However, we also anticipate the challenges of applying the promising outcomes of this study over various plant ecosystems to model GPP spatially explicitly from optical parameters and to test its robustness for different environmental factors. Nevertheless we propose the sun-induced fluorescence yield signal being a promising candidate for a RS parameter that can be used over a variety of plant ecosystems to quantify LUE directly.

Research in this field is currently strongly supported by the selection of the FLEX mission as one of ESA's candidate missions for a future Earth Explorer (Rascher, 2007; Rascher & Pieruschka, in press). Several measurement campaigns are currently under way to evaluate the accuracy by which sun-induced fluorescence can be used to quantify photosynthetic efficiency and stresses (see e.g. http://www.esa.int/esaLP/SEMQACHYX3F_index_0.html). Based on the outcome of these campaigns, it is likely that satellite-based quantification of sun-induced fluorescence yield will become a powerful tool for better understanding spatio-temporal variations of fluorescence yield, photosynthetic efficiency and distribution of plant stresses on a global scale and this way of GPP and carbon uptake.

Acknowledgements

This work was supported by a grant of the ESA in the frame of the CEFLES2 campaign (grant no. 20802/07/LG). We also thank Remo Bianchi and Michael Berger for their organizational support. The authors acknowledge Giovanni Agati (CNR-IFAC, Florence), Roberto Colombo (UNIMIB, Milan), Gloria Fernandez, Luis Alonso and Jordi Garcia (RSU, University of Valencia), Alessandro Zaldei and Piero Toscano (CNR-IBIMET, Florence), Jonas Franke (University of Bonn) and Marion Stellmes (University of Trier) for there valuable help during the field campaigns. The authors are also thankful to the two anonymous reviewers who provided constructive comments to improve this manuscript.

References

Alonso L, Gómez-Chova L, Vila-Francés J, Amorós-López J, Guanter L, Calpe J, Moreno J (2008) Improved fraunhofer line discrimination method for vegetation fluorescence quantification. *IEEE Geoscience and Remote Sensing Letters*, **5**, 620–624.

ASD (2002) *Fieldspec™ Pro Users Guide*. Analytical Spectral Devices Inc., Boulder, CO.

Aubinet M, Grelle A, Ibrom A *et al*. (2000) Estimates of the annual net carbon and water exchange of forests: the euroflux methodology. *Advances in Ecological Research*, **30**, 113–175.

Baker NR (2008) Chlorophyll fluorescence: a probe of photosynthesis in vivo. *Annual Reviews – Plant Biology*, **59**, 89–113.

Baldocchi D, Falge E, Gu LH *et al*. (2001) Fluxnet: a new tool to study the temporal and spatial variability of ecosystem-scale carbon dioxide, water vapor, and energy flux densities. *Bulletin of the American Meteorological Society*, **82**, 2415–2434.

Baldocchi DD (2003) Assessing the eddy covariance technique for evaluating carbon dioxide exchange rates of ecosystems: past, present and future. *Global Change Biology*, **9**, 479–492.

Barton CVM, North PRJ (2001) Remote sensing of canopy light use efficiency using the photochemical reflectance index – model and sensitivity analysis. *Remote Sensing of Environment*, **78**, 264–273.

Bilger W, Schreiber U, Bock M (1995) Determination of the quantum efficiency of photosystem ii and of non-photochemi-

cal quenching of chlorophyll fluorescence in the field. *Oecologia*, **102**, 425–432.

Bjorkman O, Demmig B (1987) Photon yield of O_2 evolution and chlorophyll fluorescence characteristics at 77-k among vascular plants of diverse origins. *Planta*, **170**, 489–504.

Carter GA, Theisen AF, Mitchell RJ (1990) Chlorophyll fluorescence measured using the Fraunhofer line-depth principle and relationship to photosynthetic rate in the field. *Plant, Cell and Environment*, **13**, 79–83.

Chen JM, Liu J, Cihlar J, Goulden ML (1999) Daily canopy photosynthesis model through temporal and spatial scaling for remote sensing applications. *Ecological Modelling*, **124**, 99–119.

Cohen WB, Maiersperger TK, Yang ZQ (2003) Comparisons of land cover and LAI estimates derived from ETM + and MODIS for four sites in North America: a quality assessment of 2000/2001 provisional MODIS products. *Remote Sensing of Environment*, **88**, 256–270.

Coops NC, Black TA, Jassal RPS, Trofymow JAT, Morgenstern K (2007) Comparison of MODIS, eddy covariance determined and physiologically modelled gross primary production (GPP) in a douglas-fir forest stand. *Remote Sensing of Environment*, **107**, 385–401.

Demmig-Adams B, Adams WW (1996) The role of xanthophyll cycle carotenoids in the protection of photosynthesis. *Trends in Plant Science*, **1**, 21–26.

Drolet GG, Middleton EM, Huemmrich KF *et al*. (2008) Regional mapping of gross light-use efficiency using MODIS spectral indices. *Remote Sensing of Environment*, **112**, 3064–3078.

Ehleringer J (1981) Leaf absorptances of mohave and sonoran desert plants. *Oecologia*, **49**, 366–370.

Eiden M, van der Linden S, Schween J *et al*. (2007) *Elucidating the interaction of plants in the carbon dioxide cycle using airborne hyperspectral reflectance measurements in synopsis with eddy covariance data. In: 10th International Symposium on Physical Measurements and Signatures in Remote Sensing*, Davos, Switzerland.

Field CB, Randerson JT, Malmstrom CM (1995) Global net primary production – combining ecology and remote sensing. *Remote Sensing of Environment*, **51**, 74–88.

Franck F, Juneau P, Popovic R (2002) Resolution of the photosystem i and photosystem ii contributions to chlorophyll fluorescence of intact leaves at room temperature. *Biochimica Et Biophysica Acta–Bioenergetics*, **1556**, 239–246.

Freedman A, Cavender-Bares J, Kebabian PL, Bhaskar R, Scott H, Bazzaz FA (2002) Remote sensing of solar-excited plant fluorescence as a measure of photosynthetic rate. *Photosynthetica*, **40**, 127–132.

Gamon JA, Filella I, Penuelas J (1993) The dynamic 531-nanometer reflectance signal: a survey of twenty angiosperm species. In: *Photosynthetic Responses to the Environment* (eds Yamamoto HY, Smith CM), pp. 172–177. American Society of Plant Physiologists, Rockville.

Gamon JA, Penuelas J, Field CB (1992) A narrow-waveband spectral index that tracks diurnal changes in photosynthetic efficiency. *Remote Sensing of Environment*, **41**, 35–44.

Genty B, Briantais JM, Baker NR (1989) The relationship between the quantum yield of photosynthetic electron-transport and quenching of chlorophyll fluorescence. *Biochimica Et Biophysica Acta*, **990**, 87–92.

Goel NS (1989) Inversion of canopy reflectance models for estimation of biophysical parameters from reflectance data. In: *Theory and Applications of Optical Remote Sensing* (ed. Asrar G), pp. 205–251. Wiley & Sons, New York.

Goetz SJ, Prince SD (1999) Modelling terrestrial carbon exchange and storage: evidence and implications of functional convergence in light-use efficiency. *Advances in Ecological Research*, **28**, 57–92.

Goulden ML, Munger JW, Fan SM, Daube BC, Wofsy SC (1996) Measurements of carbon sequestration by long-term eddy covariance: methods and a critical evaluation of accuracy. *Global Change Biology*, **2**, 169–182.

Govindjee (1995) 63 years since kautsky chlorophyll-*a* fluorescence. *Australian Journal of Plant Physiology*, **22**, 711–711.

Govindjee (2004) Chlorophyll a fluorescence: a bit of basics and history. In: *Chlorophyll a Fluorescence: A Signature of Photosynthesis. Advances in Photosynthesis and Respiration*, **Vol. 19** (eds Papageorgiou GC, Govindjee), pp. 1–42. Springer, Dordrecht.

Grace J, Nichol C, Disney M, Lewis P, Quaife T, Bowyer P (2007) Can we measure terrestrial photosynthesis from space directly, using spectral reflectance and fluorescence? *Global Change Biology*, **13**, 1484–1497.

Guanter L, Alonso L, Gomez-Chova L, Amoros-Lopez J, Vila J, Moreno J (2007) Estimation of solar-induced vegetation fluorescence from space measurements. *Geophysical Research Letters*, **34**, doi: 10.1029/2007GL029289.

Guo JM, Trotter CM (2004) Estimating photosynthetic light-use efficiency using the photochemical reflectance index: variations among species. *Functional Plant Biology*, **31**, 255–265.

Hall FG, Hilker T, Coops NC *et al*. (2008) Multi-angle remote sensing of forest light use efficiency by observing PRI variation with canopy shadow fraction. *Remote Sensing of Environment*, **112**, 3201–3211.

Heinsch FA, Reeves M, Votava P *et al*. (2003) *Users Guide: GPP and NPP (MOD17A2/A3) Products NASA MODIS Land Algorithm*, University of Montana, Missoula, p. 57.

Hilker T, Coops NC, Hall FG, Black TA, Wulder MA, Nesic Z, Krishnan P (2008a) Separating physiologically and directionally induced changes in pri using brdf models. *Remote Sensing of Environment*, **112**, 2777–2788.

Hilker T, Coops NC, Wulder MA, Black AT, Guy RD (2008b) The use of remote sensing in light use efficiency based models of gross primary production: a review of currant status and future requirements. *Science of the Total Environment*, **404**, 411–423.

Hirasawa T, Hsiao TC (1999) Some characteristics of reduced leaf photosynthesis at midday in maize growing in the field. *Field Crops Research*, **62**, 53–62.

Hsieh CI, Katul GG, Chi TW (2000) An approximate analytical model for footprint estimation of scalar fluxes in thermally stratified atmospheric flows. *Advances in Water Resources*, **23**, 765–772.

Janzen HH (2004) Carbon cycling in earth systems – a soil science perspective. *Agriculture Ecosystems and Environment*, **104**, 399–417.

Kljun N, Kastner-Klein P, Fedorovich E, Rotach MW (2004) Evaluation of lagrangian footprint model using data from wind tunnel convective boundary layer. *Agricultural and Forest Meteorology*, **127**, 189–201.

Lichtenthaler HK (1987) Chlorophylls and carotenoids – pigments of photosynthetic biomembranes. *Methods in Enzymology*, **148**, 350–382.

Lichtenthaler HK, Rinderle U (1988) The role of chlorophyll fluorescence in the detection of stress conditions in plants. *CRC Critical Reviews in Analytical Chemistry*, **19**, S29–S85.

Louis J, Ounis A, Ducruet JM *et al*. (2005) Remote sensing of sunlight-induced chlorophyll fluorescence and reflectance of scots pine in the boreal forest during spring recovery. *Remote Sensing of Environment*, **96**, 37–48.

Maier SW, Günther KP, Stellmes M (2003) Sun-induced fluorescence: a new tool for precision farming. In: *Digital Imaging and Spectral Techniques: Applications to Precision Agriculture and Crop Physiology*, **Vol. 66** (eds McDonald M, Schepers J, Tartly L, van Toai T, Major D), pp. 209–222. ASA Special Publication, Madison, WI, USA.

Maxwell K, Johnson GN (2000) Chlorophyll fluorescence – a practical guide. *Journal of Experimental Botany*, **51**, 659–668.

Meroni M, Colombo R (2006) Leaf level detection of solar induced chlorophyll fluorescence by means of a subnanometer resolution spectroradiometer. *Remote Sensing of Environment*, **103**, 438–448.

Meroni M, Picchi V, Rossini M *et al*. (2008a) Leaf level early assessment of ozone injuries by passive fluorescence and photochemical reflectance index. *International Journal of Remote Sensing*, **29**, 5409–5422.

Meroni M, Rossini M, Picchi V, Panigada C, Cogliati S, Nali C, Colombo R (2008b) Assessing steady-state fluorescence and PRI from hyperspectral proximal sensing as early indicators of plant stress: the case of ozone exposure. *Sensors*, **8**, 1740–1754.

Methy M (2000) Analysis of photosynthetic activity at the leaf and canopy levels from reflectance measurements: a case study. *Photosynthetica*, **38**, 505–512.

Monteith JL (1972) Solar-radiation and productivity in tropical ecosystems. *Journal of Applied Ecology*, **9**, 747–766.

Monteith JL (1977) Climate and efficiency of crop production in Britain. *Philosophical Transactions of the Royal Society of London Series B–Biological Sciences*, **281**, 277–294.

Moya I, Camenen L, Evain S *et al*. (2004) A new instrument for passive remote sensing: 1. Measurements of sunlight-induced chlorophyll fluorescence. *Remote Sensing of Environment*, **91**, 186–197.

Nichol C, Lloyd J, Shibistova O *et al*. (2002) Remote sensing of photosynthetic-light-use efficiency of a siberian boreal forest. *Tellus Series B–Chemical and Physical Meteorology*, **54**, 677–687.

Ozanne CMP, Anhuf D, Boulter SL *et al*. (2003) Biodiversity meets the atmosphere: a global view of forest canopies. *Science*, **301**, 183–186.

Papale D, Valentini A (2003) A new assessment of european forests carbon exchanges by eddy fluxes and artificial neural network spatialization. *Global Change Biology*, **9**, 525–535.

Plascyk JA (1975) Mk II Fraunhofer Line Discriminator (FLD-II) for airborne and orbital remote-sensing of solar-stimulated luminescence. *Optical Engineering*, **14**, 339–346.

Rascher U (2007) Flex-fluorescence explorer: a remote sensing approach to quantify spatio-temporal variations of photosynthetic efficiency from space. *Photosynthesis Research*, **91**, 293–294.

Rascher U, Nedbal L (2006) Dynamics of photosynthesis in fluctuating light – commentary. *Current Opinion in Plant Biology*, **9**, 671–678.

Rascher U, Nichol CL, Small C, Hendricks L (2007) Monitoring spatio-temporal dynamics of photosynthesis with a portable hyperspectral imaging system. *Photogrammetric Engineering and Remote Sensing*, **73**, 45–56.

Rascher U, Pieruschka R Spatio-temporal variations of photosynthesis – the potential of optical remote sensing to better understand and scale light use efficiency and stresses of plant ecosystems. *Precision Agriculture*, **9**, 355–366.

Reichstein M, Falge E, Baldocchi D *et al*. (2005) On the separation of net ecosystem exchange into assimilation and ecosystem respiration: review and improved algorithm. *Global Change Biology*, **11**, 1424–1439.

Reichstein M, Tenhunen JD, Roupsard O *et al*. (2002) Severe drought effects on ecosystem CO_2 and H_2O fluxes at three mediterranean evergreen sites: revision of current hypotheses? *Global Change Biology*, **8**, 999–1017.

Running SW, Nemani RR, Heinsch FA, Zhao MS, Reeves M, Hashimoto H (2004) A continuous satellite-derived measure of global terrestrial primary production. *Bioscience*, **54**, 547–560.

Schmid HP, Lloyd CR (1999) Spatial representativeness and the location bias of flux footprints over inhomogeneous areas. *Agricultural and Forest Meteorology*, **93**, 195–209.

Schreiber U, Bilger W (1993) Progress in chlorophyll fluorescence research: major developments during the past years in retrospect. *Progress in Botany*, **53**, 151–173.

Schreiber U, Bilger W, Neubauer C (1995) Chlorophyll fluorescence as a nonintrusive indicator for rapid assessment of in vivo photosynthesis. In: *Ecophysiology of Photosynthesis* (eds Schulze ED, Caldwell MM), pp. 49–70. Springer, Berlin.

Schulze ED, Caldwell MM (eds) (1995) *Ecophysiology of Photosynthesis. Ecological Studies*. Springer-Verlag, Berlin.

Schurr U, Walter A, Rascher U (2006) Functional dynamics of plant growth and photosynthesis – from steady-state to dynamics – from homogeneity to heterogeneity. *Plant, Cell and Environment*, **29**, 340–352.

Sims DA, Luo HY, Hastings S, Oechel WC, Rahman AF, Gamon JA (2006) Parallel adjustments in vegetation greenness and ecosystem CO_2 exchange in response to drought in a southern California chaparral ecosystem. *Remote Sensing of Environment*, **103**, 289–303.

Tollenaar M, Daynard TB (1978) Leaf senescence in short-season maize hybrids. *Canadian Journal of Plant Science*, **58**, 869–874.

Turner DP, Ritts WD, Cohen WB *et al*. (2003a) Scaling gross primary production (GPP) over boreal and deciduous forest landscapes in support of MODIS GPP product validation. *Remote Sensing of Environment*, **88**, 256–270.

Turner DP, Ritts WD, Cohen WB *et al*. (2005) Site-level evaluation of satellite-based global terrestrial gross primary production and net primary production monitoring. *Global Change Biology*, **11**, 666–684.

Turner DP, Urbanski S, Bremer D, Wofsy SC, Meyers T, Gower ST, Gregory M (2003b) A cross-biome comparison of daily light use efficiency for gross primary production. *Global Change Biology*, **9**, 383–395.

Valentinuz OR, Tollenaar M (2004) Vertical profile of leaf senescence during the grain-filling period in older and newer maize hybrids. *Crop Science*, **44**, 827–834.

van der Tol C, Verhoef W, Rosema A (2009) A model for chlorophyll fluorescence and photosynthesis at leaf scale. *Agricultural and Forest Meteorology*, **149**, 96–105.

Webb EK, Pearman GI, Leuning R (1980) Correction of flux measurements for density effects due to heat and water-vapour transfer. *Quarterly Journal of the Royal Meteorological Society*, **106**, 85–100.

Wofsy SC, Goulden ML, Munger JW *et al*. (1993) Net exchange of CO_2 in a midlatitude forest. *Science*, **260**, 1314–1317.

Zarco-Tejada PJ, Miller JR, Pedros R, Verhoef W, Berger M (2006) Fluormodgui v3.0: a graphic user interface for the spectral simulation of leaf and canopy chlorophyll fluorescence. *Computers and Geosciences*, **32**, 577–591.

Zhanqing L, Moreau L (1995) A new approach for remote sensing of canopy-absorbed photosynthetically active radiation. I: total surface absorption. *Remote Sensing of Environment*, **55**, 175–191.